
Theses and Dissertations

2012

Static compressive stress induces mitochondrial oxidant production in articular cartilage

Marc James Brouillette
University of Iowa

Copyright 2012 Marc James Brouillette

This thesis is available at Iowa Research Online: <http://ir.uiowa.edu/etd/2445>

Recommended Citation

Brouillette, Marc James. "Static compressive stress induces mitochondrial oxidant production in articular cartilage." MS (Master of Science) thesis, University of Iowa, 2012.
<http://ir.uiowa.edu/etd/2445>.

Follow this and additional works at: <http://ir.uiowa.edu/etd>



Part of the [Biomedical Engineering and Bioengineering Commons](#)

STATIC COMPRESSIVE STRESS INDUCES MITOCHONDRIAL OXIDANT
PRODUCTION IN ARTICULAR CARTILAGE

by

Marc James Brouillette

A thesis submitted in partial fulfillment
of the requirements for the
Master of Science degree in Biomedical Engineering
in the Graduate College of
The University of Iowa

May 2012

Thesis Supervisor: Professor James A. Martin

Copyright by
MARC JAMES BROUILLETTE
2012
All Rights Reserved

Graduate College
The University of Iowa
Iowa City, Iowa

CERTIFICATE OF APPROVAL

MASTER'S THESIS

This is to certify that the Master's thesis of

Marc James Brouillette

has been approved by the Examining Committee
for the thesis requirement for the Master of Science
degree in Biomedical Engineering at the May 2012 graduation.

Thesis Committee:

James Martin, Thesis Supervisor

Nicole Grosland

Prem Ramakrishnan

Todd McKinley

Tae-Hong Lim

Dedicated to Rachel Christine Bottjen

ACKNOWLEDGMENTS

This work was completed with tremendous help from far too many people to completely list here. However, I would like to thank a few here.

The first would be my parents, without their constant support and belief in me throughout my life, I would not be who or where I am today.

I would also like to thank all of my undergraduate professors and research mentors at Iowa State University. Drs. John Robyt and Rup Mukerjea guided me through my first personal research project where I learned the time commitments of research. Drs. Libuse Brachova, and Ludmilla Rizshsky instilled me with critical scientific habits and techniques. Working under them solidified my interest in scientific research. Finally, I would like to thank my academic advisor Desiree Gunning, who motivated me to achieve and grasp for more out of scholarly experiences.

Everyone at the University of Iowa has continued the trend of creating a helpful and learning environment for me. I would like to thank all of them. My thesis supervisor, Dr. James Martin, gave me the opportunity to continue pursuing research. Dr. Prem Ramakrishnan always helped me work through any questions or ideas. Abigail Lehman always helped out, regardless of how busy she was. Thanks also to Brice Journot, Hongjun Zheng, Barbara Laughlin, and Lei Ding for all they have taught me. I would also like to thank everyone on my committee who provided me guidance and direction at the University of Iowa.

Lastly I would like to thank Rachel Bottjen, who has sacrificed so much to help me achieve what I have

ABSTRACT

While mechanical loading is essential for articular cartilage homeostasis, it also plays a central role in the etiology of osteoarthritis. The mechanotransduction events underlying these dual effects, however, remain unclear. Previously, we have shown that lethal amounts of reactive oxygen species (ROS) were liberated from mitochondrial complex 1 in response to a mechanical insult. The sensitivity of this response to an actin polymerase inhibitor, cytochalasin B, indicated a link between ROS release and cytoskeletal distortion caused by excessive compressive strain. It did not, however, rule out the possibility that ROS may also mediate the beneficial effects of normal stresses that induce lower tissue strains required for proper homeostasis. If this possibility is true, one would expect the amount of ROS released in loaded cartilage to be positively correlated with the level of strain, and ROS should only reach lethal levels under super-physiological deformations. To test this hypothesis, full cartilage tissue strains were measured in cartilage explants subjected to static normal stresses of 0, 0.1, 0.25, 0.5, and 1.0 MPa. After compression, the percentage of ROS-producing cells was measured using the oxidation-sensitive fluorescent probe, dihydroethidium, and confocal microscopy. In support of our theory, the percentage of fluorescing cells increased linearly with increasing strains (0-75%, $r^2 = 0.8$, $p < 0.05$). Additionally, hydrostatic stress, which causes minimal tissue strain, induced minimal ROS release. In terms of cell viability, cartilage explants compressed with strains $\geq 40\%$ experienced substantial cell death, while explants with strains $<40\%$ did not. Rotenone and cytochalasin B significantly decreased ROS at 0.25 MPa, confirming that the source of ROS was the same as in the mechanical insult model. These findings demonstrated a dose-response

relationship between ROS release and whole cartilage tissue strain, and implicate mitochondria-derived ROS in mechanotransduction across a wide range of stress levels, including those in the physiological range.

TABLE OF CONTENTS

LIST OF FIGURES	vii
LIST OF EQUATIONS	viii
CHAPTER	
1. INTRODUCTION	1
2. ARTICULAR CARTILAGE BACKGROUND AND SIGNIFICANCE	3
2.1 Structure	3
2.2 Zonal distribution	4
2.3 Pericellular Matrix	5
2.4 Extra Cellular Matrix Receptors	6
2.5 Cytoskeleton	7
2.6 Mitochondria	9
2.7 Loading Articular Cartilage	10
2.8 Articular Cartilage Reactive Oxygen Species	12
2.9 Significance and Objective	14
3. MATERIALS AND METHODS	15
3.1 Articular Cartilage Explant Harvest	15
3.2 Mechanical Loading	15
3.2.1 Compression Apparatus	15
3.2.2 Hydrostatic Apparatus	16
3.3 Imaging and Quantification	16
3.3.1 Confocal Imaging	16
3.3.2 Image Analysis	18
3.4 Study 1: Oxidative Stress	18
3.5 Study 2: Compressive Stress Viability	19
3.6 Study 3: Rotenone	19
3.7 Study 4: Cytochalasin B	20
3.8 Statistical Analysis	20
4. RESULTS	21
5. DISCUSSION	28
6. REFERENCES	32

LIST OF FIGURES

Figure	
1. Schematic of cartilage structure and fibril orientation.....	5
2. Three-dimensional reconstructions from confocal laser scanning microscopy (CLSM) of cartilage sections labeled for actin microfilaments (A,D,G), - tubulin (B,E,H), and vimentin (C,F,I) from the different depth zones: tangential (A-C), transitional (D-F), and radial (G-I).	8
3. Sites of mitochondrial ROS, with inhibitors listed in red.....	10
4. Mechanical loading devices. (A) Device for compressive stress shown in a low oxygen incubator. The inset shows an osteochondral explant submerged in culture medium in the housing under the compression platen. (B) Hydrostatic device shown in a water bath. The inset shows an explant sealed in a plastic bag containing culture medium. The bag is submerged under water in the unit.	17
5. Representative picture of explant in screw fixation.....	18
6. Representative z-axis stacked confocal images (20x objective) showing oxidant producing (Red) and live cells (Green) after static compressive stress with 0 MPa (A), 0.1 MPa (B), 0.25 MPa (C), 0.5 MPa (D), and 1.0 MPa (E). The bar in A indicates 40 microns	22
7. Percentage of cells stained with oxidative marker dihydroethidium (DHE) and cell death percentage (DEAD) under various static compressive stresses applied (*p<0.05).....	23
8. DHE staining and mechanical strain. Linear regression analysis revealed a strong linear relationship between DHE and strain, which increased together over the range from 0 to >75% strain... ..	24
9. Effects of hydrostatic stress on DHE staining. Hydrostatic stresses (HS) of 0.5 MPa and 1.0 MPa resulted in significantly lower oxidant levels in comparison with 0.5MPa and 1.0MPa of static compressive stress (* p<0.05).....	26
10. Effects of rotenone and cytochalasin B on stress-induced DHE staining. Inhibition of Mitochondrial electron transport with rotenone decreased oxidant production (% DHE stained cells) after 0.25MPa and 0.5MPa of static compressive stress. Cytoskeletal dissolution with cytochalasin B (Cyto B) significantly decreased DHE at 0.25MPa (* p<0.05) but no reduction was discerned at 0.5MPa.....	27

LIST OF EQUATIONS

Equation

1. Percentage DHE stained cells14

CHAPTER 1

INTRODUCTION

The material properties of articular cartilage are well suited to resist normal physiological stresses in joints. This favorable structure and composition develops in response to mechanical cues and depends on mechanical stimulation for stability [2]. Mechanical stress-induced deformation of the cartilage extracellular matrix (ECM) is sensed by resident chondrocytes via integrin-mediated attachments to collagens, fibronectin, and other matrix components. Integrin signaling can either maintain or degenerate the ECM by increasing biosynthetic activity or protease activity, respectively. In general, normal loading conditions result in physiological strains that promote cell viability and biosynthetic activity, whereas super-physiological strains from injurious loads are deleterious and can lead to progressive cartilage degeneration, the hallmark of osteoarthritis (OA) [3-6]. The mechanotransduction pathways driving these divergent effects are unknown, but there is evidence to suggest that mechanical stresses modulate the production and release of reactive oxygen species (ROS) by chondrocytes, which in turn regulate energy metabolism [7, 8].

Despite near exclusive reliance on glycolysis for ATP, cartilage chondrocytes do harbor mitochondria, and mitochondrial dysfunction has been implicated in the development of osteoarthritis [9-14]. It has been estimated that under normal conditions, 2-3% of molecular oxygen is incompletely reduced to $O_2^{\bullet -}$. This level of superoxide is sufficient for intracellular signaling and other processes, but does not cause extensive oxidative damage [15]. Previous work has shown that an injurious level of mechanical

stress leads to a lethal burst of oxidants from complex 1 of the electron transport chain, resulting in a near 70% loss of chondrocytes [16]. These findings implicate mitochondrial-derived ROS in cartilage response to excessive stress, but do not exclude the possibility that ROS could play a fundamental role in normal cartilage mechanotransduction pathways as well, which has been found to be produced at physiological loading conditions [7].

Mitochondria are attached to the cytoskeleton via interaction with F-actin, which facilitates their motility and stability [17]. In articular chondrocytes, this physical connection with the cytoskeleton exposes the mitochondria to distortion as the ECM is deformed by mechanical stress [18]. In a cartilage injury model, dissolution of cytoskeletal proteins, using cytochalasin B or nocodazole prior to impact, mitigated ROS production and chondrocyte mortality [19]. These findings suggest a link between mechanical stress and intracellular ROS production.

Taken together, these studies hint that mitochondrial-derived ROS are produced in response to both injurious and physiological loading. Therefore, ROS production should be proportional to tissue strain and remain sub-lethal within normal strain range. To test this, we measured tissue strain, ROS production, and chondrocyte viability in osteochondral specimens exposed to increasing static compressive (0.1- 1.0 MPa) and hydrostatic (0.5-1.0 MPa) stresses. The loading response effects of rotenone or cytochalasin B were also tested to confirm mitochondrial and cytoskeletal involvement in strain-related ROS production.

CHAPTER 2

ARTICULAR CARTILAGE BACKGROUND AND SIGNIFICANCE

2.1 Structure

Articular cartilage is the synovial joint-covering tissue responsible for absorbing and transmitting the mechanical loads imposed by the body. It is a uniquely thin tissue (1-3mm) that endures continuous and repetitive stresses, while allowing near frictionless articulations and translations of the various joints. Articular cartilage, once thought to be a static substance with no reparative capabilities as an avascular and alymphatic tissue, is now known to be dynamic and responsive to the various environmental stimuli to which it is exposed.

Although articular cartilage is mostly water by weight (65-85%) [20] the structure is primarily defined by a dense extracellular matrix (ECM) composed of collagens, proteoglycans, and glycoproteins; the two main constituents being collagen and aggrecan. Only a single cell type exists within this tissue: the chondrocyte. These cells comprise only about one percent of the total tissue volume, but are entirely responsible for maintaining the ECM around them [21].

Collagen creates the major framework from which all other structures attach, accounting for ~50% of cartilage's dry weight and being principally responsible for the tissue's tensile strength [22]. These collagen fibrils are predominantly type II collagen, although collagens III, VI, IX, X, XI, XII, and XIV are also present [23-25]. The fibril diameter of type II collagen directly depends on the number of small leucine rich repeat proteoglycans (SLRPs) incorporated into the structure, most notably decorin, during fibril

formation [25]. These SLRPs are also thought to limit cleavage site access to collagenases, together providing both structural protection and diameter control [26].

Aggrecan, the other main constituent of articular cartilage, is a proteoglycan composed of a core protein with glycosaminoglycan (GAG) attachment sites for chondroitin sulfate and keratan sulfate [26]. Aggrecan exists as large aggregates rather than independent molecules [27], and forms as aggrecan binds to hyaluronic acid (HA) via link protein [26]. The GAG attachments provide an anionic environment for water binding [25, 26], although only partial hydration of these GAG side chains is achieved due to steric hindrances from the collagen network. This arrangement creates swelling pressure which provides articular cartilage with compressive strength [25].

2.2 Zonal Distribution

The tissue is divided into the following four zones from the outside-in: superficial (tangential), middle (transitional), deep (radial), and calcified cartilage [2, 28]. The distinction of these zones is loosely based on cell and collagen fibril orientation relative to the articulating surface. Collagen fibrils are parallel in the superficial zone, random in the middle zone, and perpendicular in the deep zone [29, 30]. This organization is not random, but instead serves a functional role in each zone of cartilage [25].

Because the superficial zone receives the highest shear stress from joint articulation, the chondrocytes are flattened, stretching parallel to the surface [22, 25]. Here the aggrecan concentration is at its lowest, and the collagen fibers have their smallest diameter (20nm) [25, 31-33] due to the fact that decorin, a fibril associated SLRP, is at its highest concentration as along with the proteoglycan, biglycan [34]. Even with this collection of smaller actin filaments, the superficial zone still has the highest

tensile strength of all the zones [25, 31-33]. The chondrocytes are also unique here as they produce lubricin, a protein that alleviates most of the friction associated with joint articulation [35]. In the middle zone, cell density is lower, and the chondrocytes produce collagen type II and aggrecan [22, 25]. The deep zone has the lowest cell density of all, but also has the highest collagen fibril diameter (70-120nm) [33] and aggrecan concentration [33].

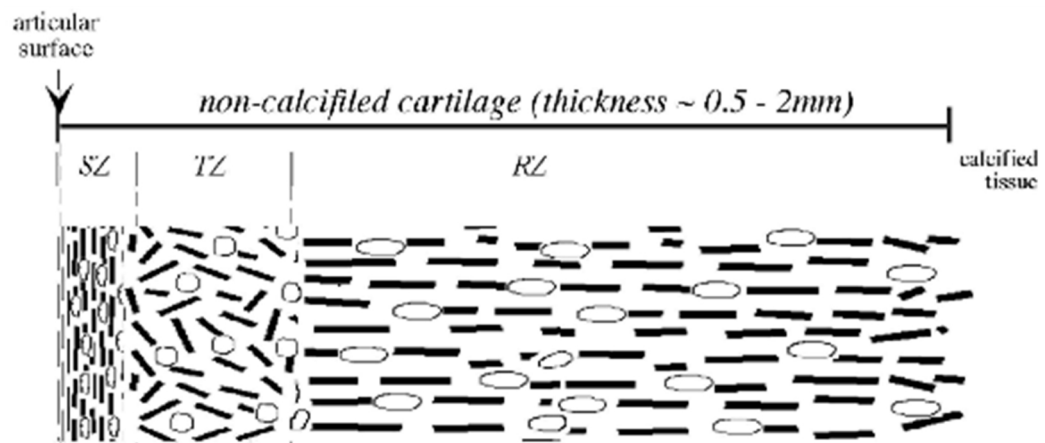


Figure 1. Schematic of cartilage structure and fibril orientation [36].

2.3 Pericellular Matrix

The small region of the ECM immediately surrounding each chondrocyte is called the pericellular matrix (PCM). This area is associated with having a higher proteoglycan content and finer collagen fiber arrangement compared to the surrounding ECM [25, 37], and usually extends two microns beyond the cell. Collagens type II and IX are found in

this area, but the defining characteristic is the presence of type VI collagen, which is absent from the rest of the ECM [38-43]. Because the PCM is the immediate structure beyond the chondrocyte cell membrane, it must contain the proper cell attachments for any mechanotransduction events that will need to traverse this area for signaling [37].

2.4 Extracellular Matrix Receptors

Chondrocytes are attached to the ECM via multiple different protein receptors in order to sense the mechanical environment surrounding them. The most well-known family of receptors is the integrins, named for their integral role in linking the ECM of tissue to the cellular cytoskeleton [44, 45]. Integrins are transmembrane heterodimers composed of non-covalently bound α and β subunits. There are 18 α and 8 β subunits, which can combine to form 24 heterodimer varieties in vertebrates [46], the majority of which form links to the actin cytoskeleton [47]. Chondrocytes have been found to express integrins that bind type II and type VI collagen, laminin, bitronectin and osteopontin, and fibronectin [48-51], as the survival of these cells has been shown to depend on the binding of these protein receptors [52, 53]. The fibronectin receptor ($\alpha 5 \beta 1$) is the most abundant in chondrocytes and plays the greatest role in attachment when cultured in monolayers [48, 54]. Two other notable ECM receptors present in chondrocytes are annexins and the hyaluronan receptor, CD44 [55, 56]. Annexin V binds to type II collagen and is preferentially expressed in the superficial zone [56].

While further studies would be needed to link the effects of specific mechanical stimulation to respective receptors, it is important to state that all of the receptors chondrocytes possess have the potential for translating mechanical stimulation from external mechanical forces, such as joint loading, into an intracellular signal.

2.5 Cytoskeleton

The cytoskeleton serves three general purposes: (1) spatial organization of cell content, (2) generation of forces required for cell motion, and (3) physical connections between cells and the ECM [57]. The cytoskeleton within chondrocytes is composed of actin microfilaments, tubulin microtubules, and vimentin intermediate filaments (Fig 2) [58]. Together, these three filaments form a network within the cell to create a rigid framework for support of the cell membrane.

Actin is a widespread, 43kDa protein made up of three different monomers. These monomers form long filaments *in vivo*, and grow preferentially on their plus, or barbed, end and much slower on their minus or pointed end [59]. Actin assembly consumes ATP, the ATP bound G-actin is incorporated into the barbed end, however at the same time the ADP-Actin monomers are lost from the pointed end [59]. This constant turnover is called 'treadmilling' and is important for many cellular activities, including locomotion [60]. Cytochalasin B and D are known to prevent the growth of actin from the barbed end, and have shown to drastically decrease the rigidity of chondrocytes [61].

Like actin microfilaments, tubulin microtubules are also a globular protein. However, tubulin is dimeric rather than trimeric, with each monomer being 55kDa in size [62]. Tubulin is a GTPase, which is consumed upon assembly of the monomers onto the filament. The filament contains a faster growing plus end, just as actin did, however there is a polarization present in this filament, which is very important to its intracellular function of being the highway for shuttling material throughout the cell [63, 64].

Less is known about the intermediate filaments other than their participation in mRNA transport [65]. They are in between the size of microfilaments and microtubules.

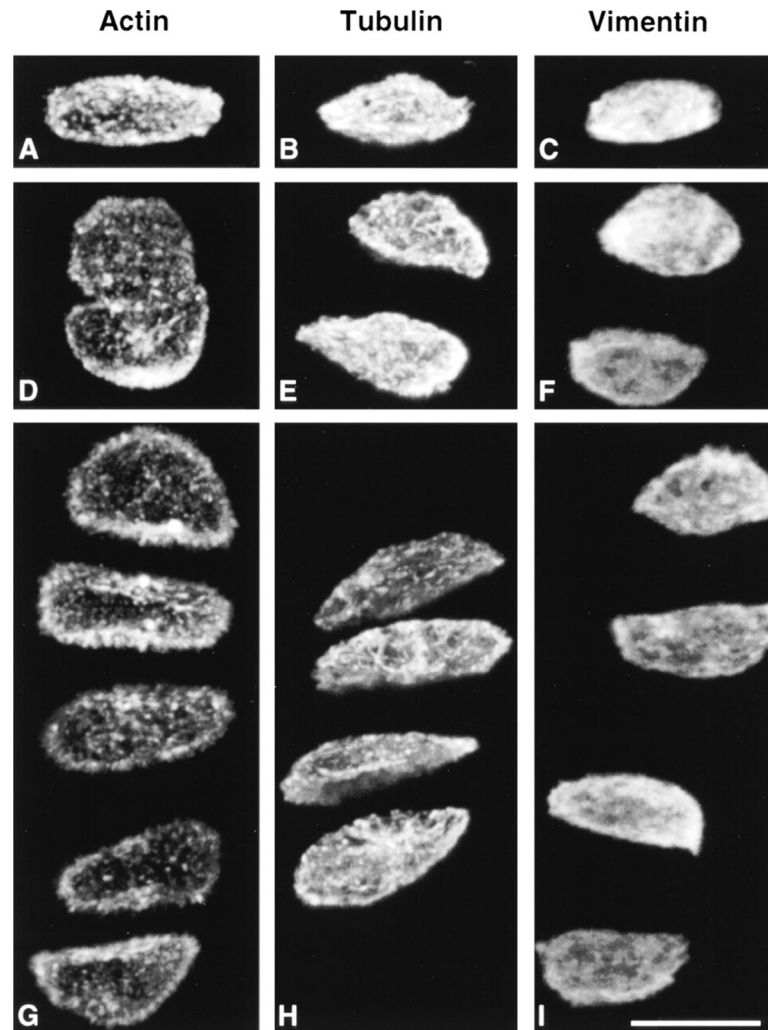


Figure 2. Three-dimensional reconstructions from confocal laser scanning microscopy (CLSM) of cartilage sections labeled for actin microfilaments (A,D,G), - tubulin (B,E,H), and vimentin (C,F,I) from the different depth zones: tangential (A-C), transitional (D-F), and radial (G-I) [66].

2.6 Mitochondria

Mitochondria are known for being the powerhouses of cells, producing an abundance of ATP through the electron transport chain. In articular cartilage, however, glycolysis is the near exclusive source of ATP. So, as one would expect from a cell that minimally utilizes oxidative phosphorylation, inhibition of ATP synthase results in no significant change in tissue-level ATP content, while glycolytic inhibitors significantly decreases it [8]. Interestingly, though, when complex I of the electron transport chain was blocked by rotenone, a decrease in ATP content was observed.

It has been demonstrated that mitochondria convert some O₂ to superoxide by incomplete reduction at complex I [15]. In articular cartilage, it is believed that this source of ROS supports glycolysis. Because the tissue exists in such a low oxygen environment, the ROS produced by mitochondria would be used to recycle glycolytic products to maintain redox balance.

The physical connection between the mitochondria and ECM has been shown to depend on both actin and microtubules because when they are depolymerized, mitochondrial displacement from stimulation is significantly reduced [67].

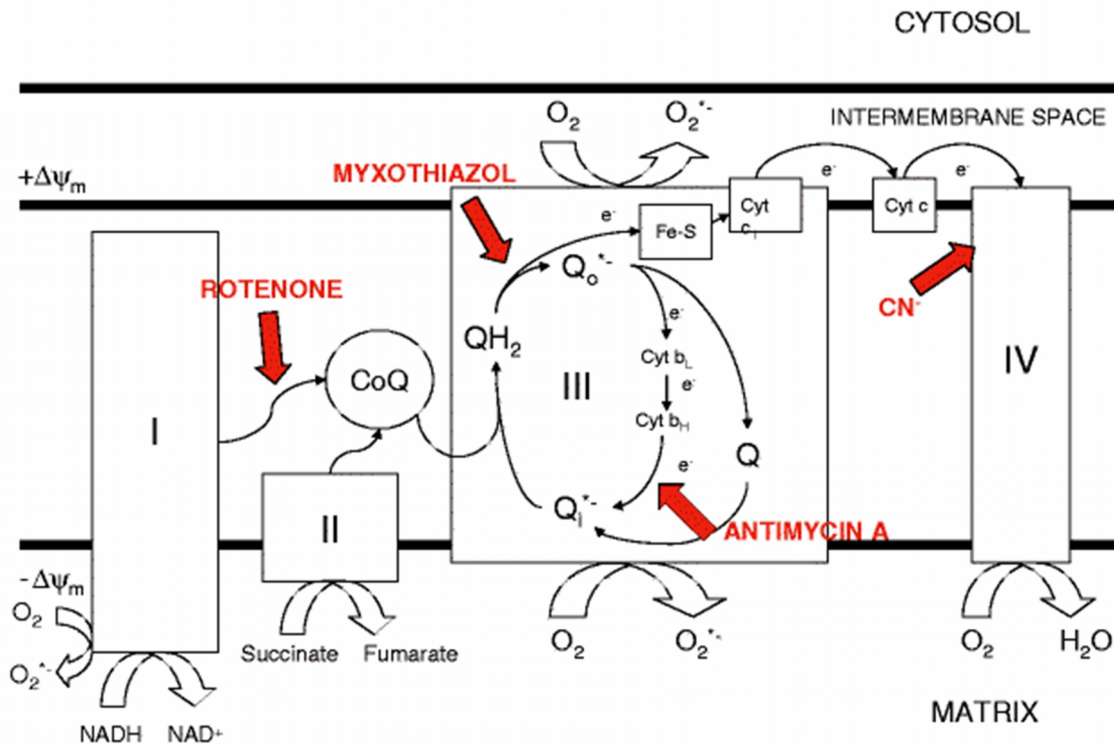


Figure 3. Sites of mitochondrial ROS, with inhibitors listed in red [1]

2.7 Loading Articular Cartilage

Articular cartilage supports the varying loads created by body motion, involving a variety of stresses onto the tissue, namely compressive, hydrostatic, and shear [68].

Since articular cartilage is responsible for absorbing these loads, the levels of these loads and their effects on cartilage, especially chondrocytes, needs to be understood.

Walking imparts body weight loads onto the joints of the lower extremities. These loads can range from 3 times body weight (BW) to 8 times BW, with larger loads occurring on a downhill slope [69, 70]. These loads impart stresses around 5MPa for 8

times BW on a healthy knee [69], however, stresses can reach 20MPa in the hip joint during stair climbing [71].

The loading of articular cartilage is necessary for inherent tissue maintenance [72, 73]. The constituents of articular cartilage have been shown to individually respond to physiological loading. For example, it has been demonstrated in canines that physiological loading increases proteoglycan (PG) content [74], and cultured implants exposed to dynamic compression have increased GAG synthesis [75]. Cytoskeletal networks also respond to mechanical loads, with integrins mediating the indirect attachment of the actin cytoskeleton to the PCM [76-79]. Cyclic and static compression of articular cartilage cells in agarose scaffolds have shown significant actin cytoskeleton reorganization, replacing the uniform cortical distribution shown in control scaffolds with a punctate organization in loaded scaffolds [80]. This actin network is also responsible for transmitting compressive distortions and cellular volume changes to intracellular compartments, such as the nucleus [81]. When the actin network is inhibited with cytochalasin D, nuclear volume is no longer affected by the compression [81].

When the loading regimes fall outside of normal, physiological ranges, catabolic effects on cartilaginous components ensue. Increased joint loading in the knee as a result of ligamentous injury results in degradative tissue changes [82]. Also, athletes who participate in high impact sports, such as basketball and soccer, have a higher prevalence of articular cartilage injuries [83, 84]. High, repetitive loads, as modeled by a canine 8-month treadmill exercise regimen, also shows that degradative changes can occur without the occurrence of a discrete injury [85].

Severely underloading articular cartilage is also hazardous. Animal models have demonstrated underloading to soften cartilage [86], reduce aggrecan and hyaluronan content [87], and decrease cell density and matrix integrity [88]. The effects of this reduced loading do not fully recover after extended immobilization [87, 89]. Similar results can be seen in human articular cartilage. Partial weight bearing over a 7 week time period resulted in knee articular cartilage thinning [90].

Hydrostatic stress is also a contributor to matrix modulation and cytoskeletal reorganization. Depending on the level, duration, and cyclic or static waveform of application, the response varies. Cyclic application of 5MPa hydrostatic pressure at 0.5Hz or static application of 5MPa resulted in actin remodeling similar to that seen after compression [80]. When the hydrostatic pressure (1, 5, 10 MPa) is applied intermittently at 1Hz for 4 days, significant increases in collagen and aggrecan mRNA levels are observed [91]. In contrast, when high stress is applied (30MPa), the actin cytoskeletal network degenerates and is associated with decreased PG synthesis [92, 93].

2.8 Articular Cartilage Reactive Oxygen Species

Oxygen is a scarcity in articular cartilage, estimated levels of O₂ stay around 5% at the superficial zone, and decrease to 2-3% in the deep zone [94-99]. Articular cartilage has adapted to this environment, as shown by the fact that both PG aggrecanation and collagen type II synthesis, are higher at oxygen concentrations near 5%. [100, 101].

Because energy in articular cartilage is primarily derived from glycolysis [8, 102], low oxygen levels do not produce an intuitive concern for its production. But when oxygen is completely deprived, negative metabolic effects do occur in cartilage, and these

effects can be rescued by external oxidant supplementation [103]. This supports the theory that although oxygen is not used directly via the electron transport chain for the majority of ATP production, it is necessary for supporting glycolysis.

The mechanism by which oxygen supports chondrocyte metabolism and matrix maintenance seems to lie in the incomplete reduction of oxygen to superoxide. When complex I of mitochondria is blocked by rotenone, ROS production is decreased, which in turn decreases proton efflux from chondrocytes [104]. This effect can be reversed by external oxidant supplementation [104]. This same relationship exists with glycolytic ATP production in chondrocytes, with ATP depending on ROS produced from the same mitochondrial source [8]. The production of these chondrocyte ROS increases with applied stress to the cartilage [7, 105]. When mechanical stress reaches levels high enough to inhibit PG synthesis, antioxidant supplementation is able to recover it [7].

The excessive stress levels seen to increase oxidant production are also present in high energy impact injuries [16]. Chondrocyte mortality caused by high energy impacts can be reduced by oxidant pretreatment [106], and post impact antioxidant treatment also imparts this chondrocyte-sparing effect [107]. These oxidant levels are dramatically decreased with pretreatment of the complex I inhibitor, rotenone, which again prevents chondrocyte death due to high energy impact.

2.9 Significance and Objective

Osteoarthritis is a debilitating disease characterized by joint pain and degradation [108]. Excess ROS is implicated in progressing this articular cartilage matrix degradation as seen by increased lipid peroxidation [109], nitric oxide and nitrotyrosine

levels [110, 111], and oxidized immunoglobulin G [112]. Also, the mechanical properties of cartilage become compromised in osteoarthritis [113-115]. Linking this information with the fact that mitochondrial distortion is dependent on the cytoskeletal connections, and ROS release is stress dependant warrants further investigation of the role that mechanical cellular stress and strain has on mitochondrial ROS production and its subsequent effects. Thus, the goal of this thesis work was to find and describe the relationship that tissue strain has with mitochondrial ROS production in bovine articular cartilage explants.

CHAPTER 3

MATERIALS AND METHODS

3.1 Articular Cartilage Explant Harvest

Osteochondral explants (15mm X 15mm) were manually harvested from mature bovine lateral tibial plateaus under sterile conditions. The subchondral bone was left attached with a thickness of 5-8mm. The explants were cultured in phenol red free culture media, which was equilibrated in low oxygen conditions (5% O₂, 5% CO₂), containing 45% Dulbecco's Modified Essential Medium (DMEM), 45% F12, 10% Fetal Bovine Serum (Invitrogen®) for 48 hours after harvest, allowing the explants to reach a biosynthetic equilibrium in culture. After equilibration, the central cartilage thickness was measured using a calibrated ultrasound device (Sonopen®, Olympus NDT).

3.2 Mechanical Loading

3.2.1. *Compression Apparatus*

Mechanical loading was achieved using a custom indentation device previously described (Fig 4) [116]. Briefly, specimens were securely fixed in a custom jig interfaced with stainless steel screw fixators with the explant completely bathed in culture media (Fig 5). Contact with the cartilage surface was initiated with an 8mm-diameter flat, non-porous cylindrical indenter prior to stress application. Cartilage was subjected to static compressive stress (creep) using a custom LabVIEW application with the loading device housed inside a low oxygen incubator(5% O₂, 5% CO₂). Cartilage thickness information and the displacement data were utilized to determine maximum total cartilage thickness

strain endured during compressive stress and correlated with viability or oxidant information.

3.2.2. *Hydrostatic Apparatus*

Cartilage explants were placed inside impermeable bags completely bathed in low oxygen equilibrated media, heat-sealed and placed inside the hydrostatic chamber. The chamber was evacuated and filled with distilled water to function as the pressurizing liquid. The hydrostatic pressure chamber was instrumented with a stepper motor (Ultramotion®, with optical encoder feedback) and pressure transducer (Sensotec® FP2000 series). Static pressure was achieved using the stepper motor to depress a hydraulic piston attached to the chamber (Fig 4). Actuator control and pressure feedback were controlled and programmed with LabVIEW.

3.3 Imaging and Quantification

3.3.1. *Confocal Imaging*

Immediately after loading, explants were stained with 5.0 μ M dihydroethidium (DHE, Invitrogen), an ROS indicator, or 1.0 μ M ethidium homodimer-2 (EthD-2, Invitrogen), a cell death indicator, along with 1.0 μ M calcein AM (Invitrogen), a live cell indicator, for 30 minutes under previously described low oxygen culture conditions. Specimens were imaged using a Bio-Rad MRC-1024 confocal microscope available at the central microscopy research facility (CMRF, University of Iowa). Images of the explants were made with a 20x water immersion lens (Nikon). Three random sites within the loading region were imaged from the surface to a depth of \sim 200 μ m in 20 μ m intervals. This yielded a z-axis stack of 11 images at each sampling location. Cell counts of the viable cells and DHE-positive cells in the z-axis stack were combined in the z-direction

to give a composite value for chondrocyte viability and DHE production for each sampling site.

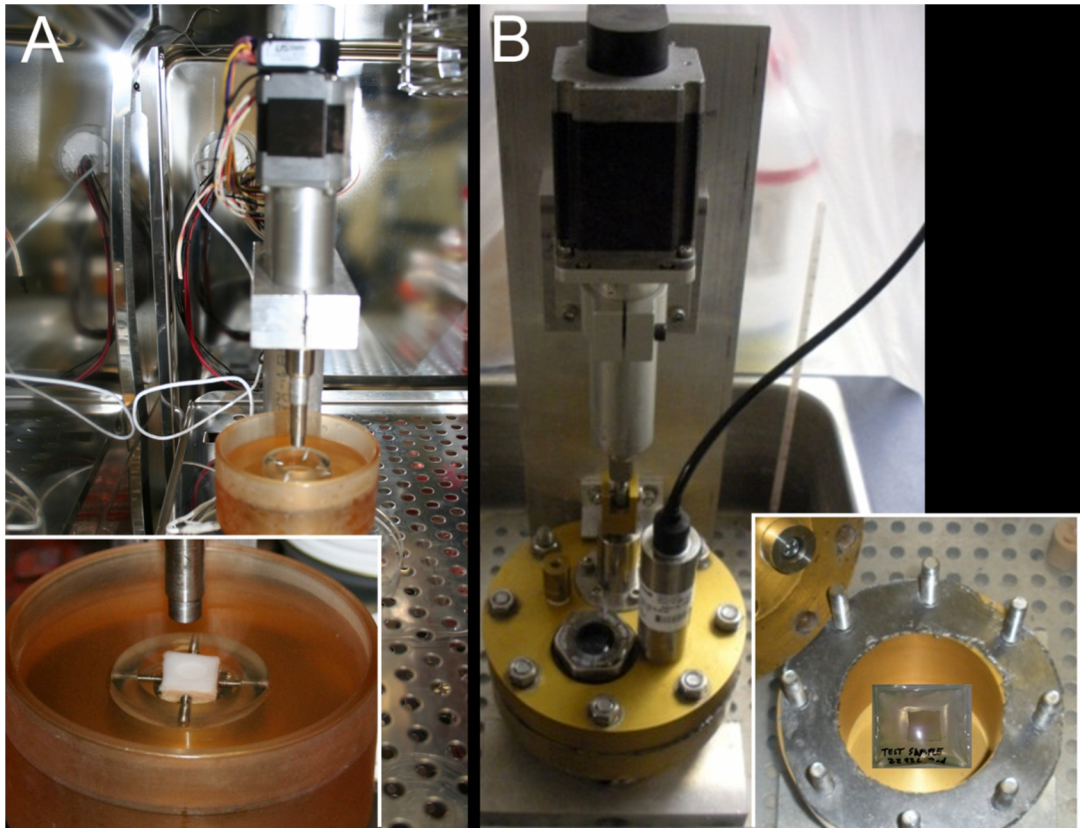


Figure 4. Mechanical loading devices. (A) Device for compressive stress shown in a low oxygen incubator. The inset shows an osteochondral explant submerged in culture medium in the housing under the compression platen. (B) Hydrostatic device shown in a water bath. The inset shows an explant sealed in a plastic bag containing culture medium. The bag is submerged under water in the unit.

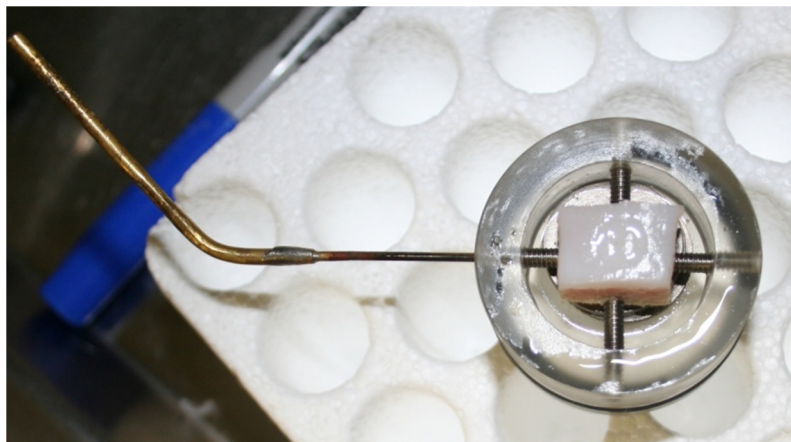


Figure 5. Representative picture of explant in screw fixation.

3.3.2. *Image Analysis*

Cell counts for oxidant production and viability were achieved using Quantitative Cell Image Processing (QCIPTM), a custom automated MATLAB® cell counting program[117]. Briefly, the automated application was designed to employ image information such as fluorescence intensity, cell boundary, and circularity information to reduce subjectivity in counting procedures. Programmed subroutines perform automatic thresholding of image slices and detect ‘out of focus’ cells to reduce counting redundancy. The program analyzes each slice in a stack of images and outputs a final count of live cells (calcein AM) and oxidant producing cells (DHE) or dead cells (EtHD-2).

3.4 Study 1: Oxidative Stress

After 48 hours in culture, cartilage thickness was measured at the center of the specimen using a calibrated ultrasound device (Sonopen®, Olympus NDT) before

mechanical loading. Explants were subjected to one of the following static compressive stresses: 1) 0 MPa, 2) 0.1 MPa, 3) 0.25 MPa, 4) 0.5 MPa, 5) 1.0 MPa. Stress application was maintained for one hour and displacements were continuously recorded. To study the effect of hydrostatic stress, explants were subjected to 0.5MPa or 1MPa for 1 hour inside the hydrostatic apparatus. Stressed explants were stained for oxidant measurement (calcein AM and DHE) and imaged. Image data were processed for oxidant and total cell counts using QCIP™. Oxidant cell counts were reported as percentage of total cells counted:

$$1. \text{ Percentage DHE stained cells} = \frac{(\text{total DHE cells})}{(\text{total DHE cells})+(\text{total calcein cells})} * 100$$

3.5 Study 2: Compressive Stress Viability

Explants were subjected to static compressive stress as described in Study 1. Explants were stained for viability assessment (calcein AM and EthD-2) and imaged. Image data were processed for dead cell and total cell counts using QCIP. Cell death cell counts were reported as percentage of total cells counted.

3.6 Study 3: Rotenone

To determine if blocking mitochondrial NADH dehydrogenase (Complex I) during static compressive stress had an effect on ROS production, explants were incubated with 2.5µM rotenone (Sigma Aldrich®) one hour prior to either 0.25MPa or

0.5MPa static compressive stress for 1 hour with continued exposure to rotenone.

Explants were stained and imaged for oxidant production (DHE and calcein AM) and reported as a percentage of total cells counted as previously described in study 1.

3.7 Study 4: Cytochalasin B

To investigate the role of the cytoskeleton in mitochondrial mechanotransduction, explants were pre-treated with 20 μ M cytochalasin B (Sigma Aldrich) four hours prior to static stress loading at 1) 0.25MPa and 2) 0.5MPa for one hour. Immediately after loading explants were stained, imaged and analyzed for oxidant production as described in study 1.

3.8 Statistical analysis:

Five explants were employed in each treatment combination containing three unique image sites. One-Way Analysis of Variance on ranks with Dunn's multiple comparison was employed to assess statistical differences in oxidant production and viability under different pretreatments and stress applications. Significance level was set at $p < 0.05$. Linear regression and Spearman rank order correlation was employed to identify any tendency of variation.

CHAPTER 4

RESULTS

Representative confocal images show calcein AM and DHE staining after static stress compression (Fig 6). It is visually apparent that the percentage of DHE-stained cells increased with increasing compressive stress, as confirmed by quantitative image analysis (Fig 7). In unloaded (control) specimens, 3.9% ($\pm 4\%$) of the cells were stained with DHE. Staining increased to 12% ($\pm 9\%$) at 0.1 MPa, 35% ($\pm 18\%$) at 0.25 MPa, 55% ($\pm 14\%$) at 0.5 MPa and 75% ($\pm 9\%$) at 1 MPa. The increases at 0.25, 0.5, and 1.0 MPa were significant ($p < 0.05$). Compressive stresses up to 0.5 MPa did not induce high cell mortality, which ranged between 4% ($\pm 3\%$) in unloaded specimens to 12% ($\pm 8\%$) in specimens loaded to 0.5 MPa. However, mortality did rise to 38% ($\pm 10\%$) with 1.0 MPa compression, a significant increase above all other doses ($p < 0.05$).

Strain values associated with static compressive stress ranged from 0% in unloaded controls to greater than 75% in explants compressed with 1.0 MPa (Fig 8). Regression analysis revealed a strong linear relationship between strain magnitude and DHE production ($R^2 = 0.80$), and the Spearman rank order test showed a positive correlation as well (0.87; $p < 0.001$).

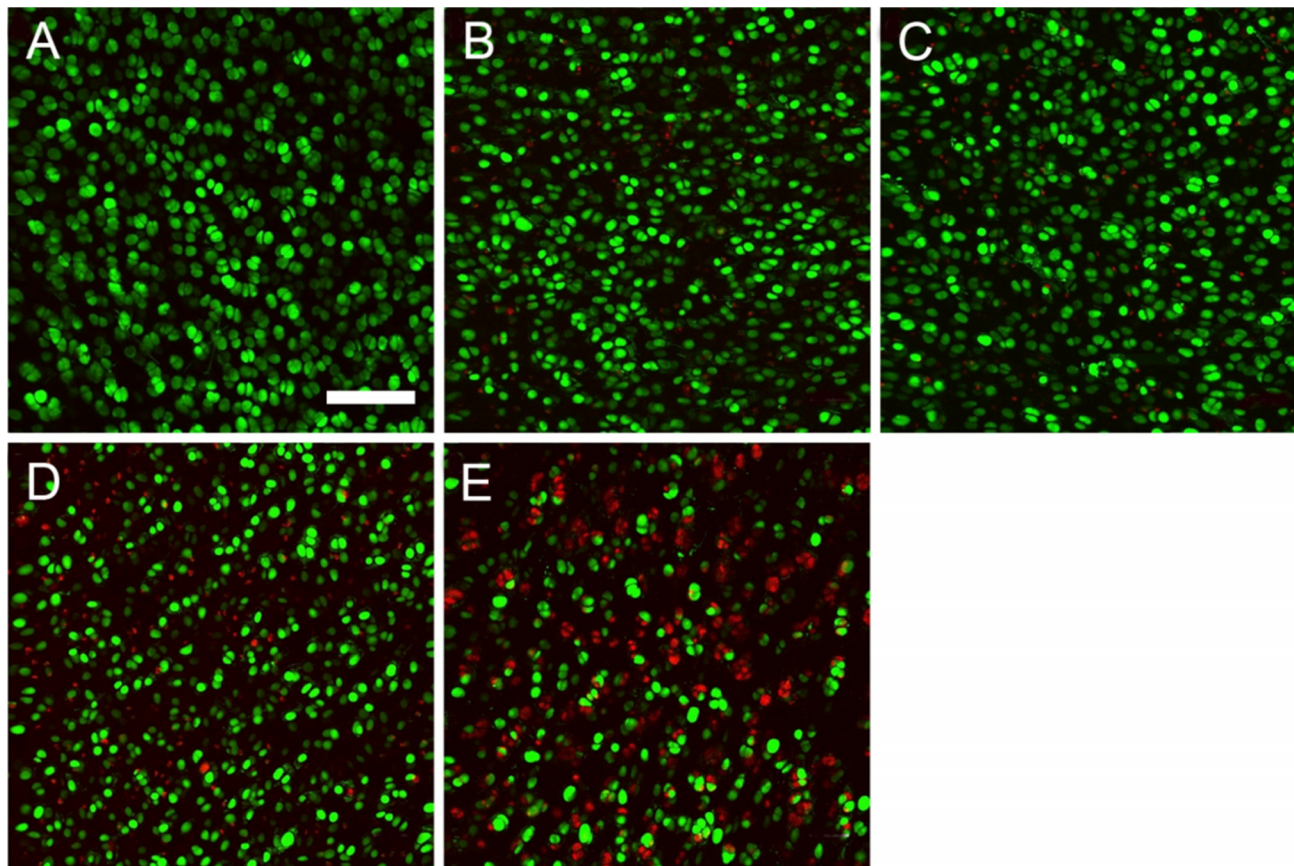


Figure 6. Representative z-axis stacked confocal images (20x objective) showing oxidant producing (Red) and live cells (Green) after static compressive stress with 0 MPa (A), 0.1 MPa (B), 0.25 MPa (C), 0.5 MPa (D), and 1.0 MPa (E). The bar in A indicates 100 microns

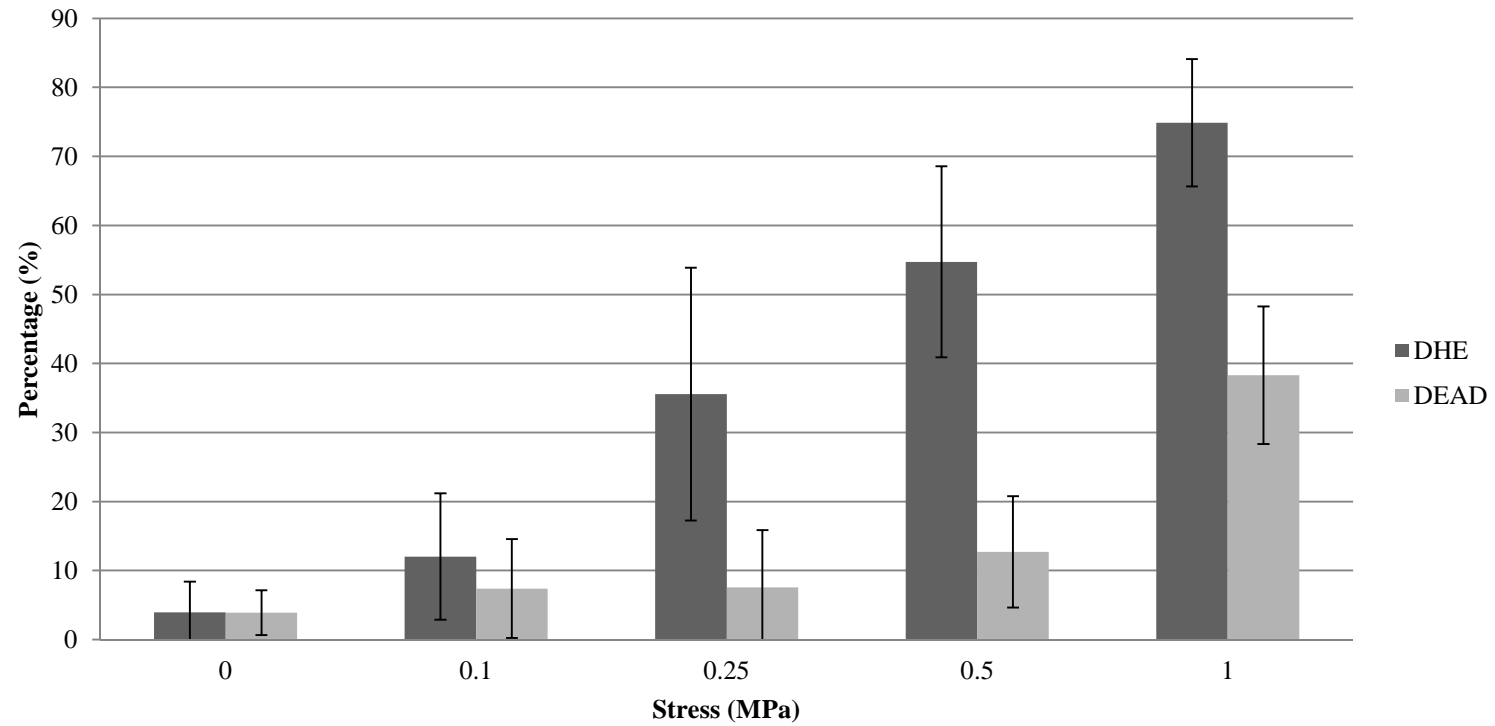


Figure 7. Percentage of cells stained with oxidative marker dihydroethidium (DHE) and cell death percentage (DEAD) under various static compressive stresses applied (* $p < 0.05$).

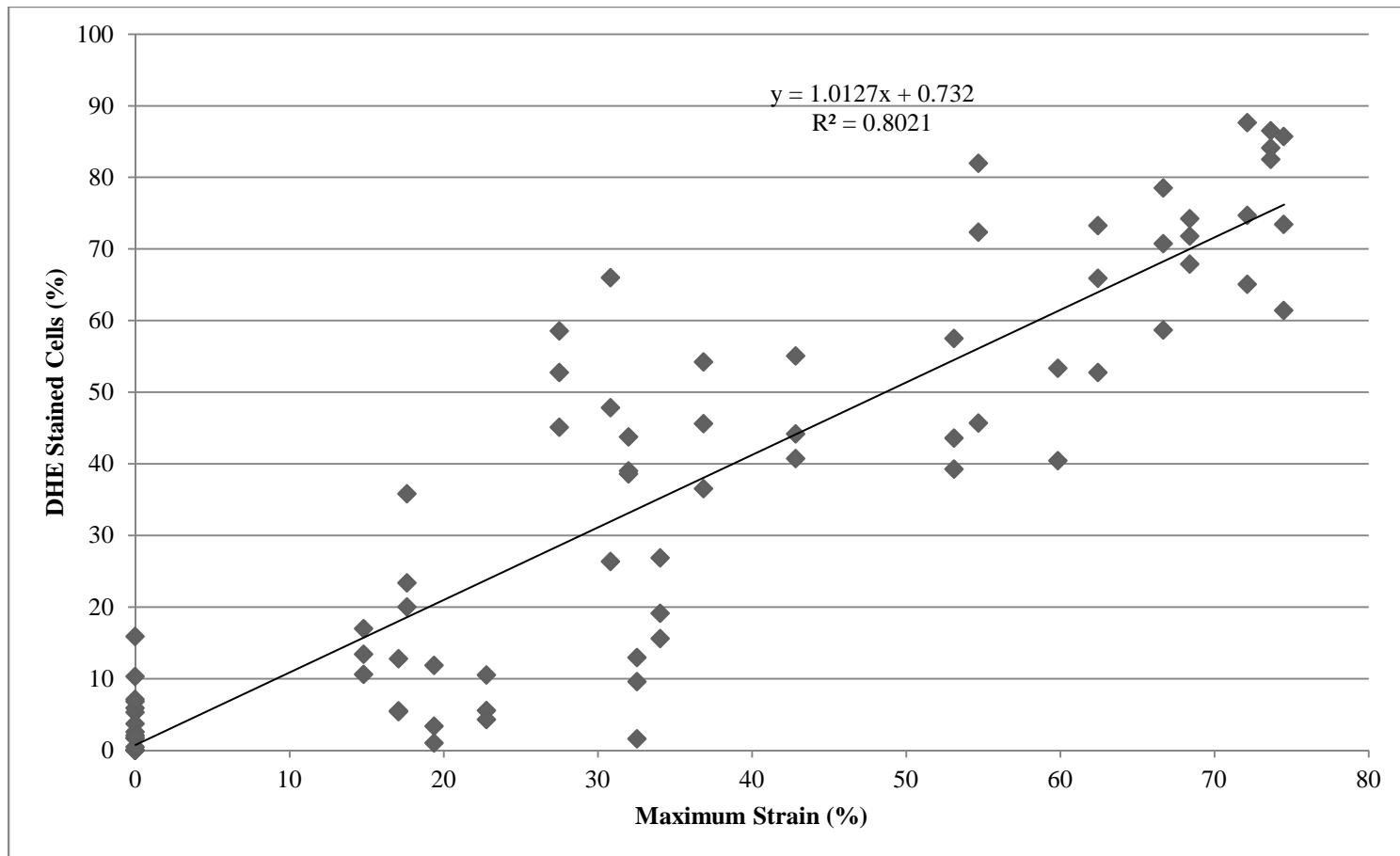


Figure 8. DHE staining and mechanical strain. Linear regression analysis revealed a strong linear relationship between DHE and strain, which increased together over the range from 0 to >75% strain.

In contrast to static compressive stress, hydrostatic stress did not provoke significant strain or increases in DHE staining at 0.5MPa ($5.3\% \pm 8\%$) or 1.0MPa ($7.9\% \pm 9\%$) (Fig 9).

Figure 10 shows that pretreatment with the mitochondrial electron transport inhibitor, rotenone, significantly reduced oxidant staining at 0.25MPa static compression ($11\% \pm 10\%$, $p < 0.05$), but did not significantly reduce staining at 0.5MPa ($41\% \pm 23\%$). Similar trends were observed when explants were pretreated with cytochalasin B, an inhibitor of actin polymerization (Fig 10): DHE staining declined significantly ($13\% \pm 14\%$) at 0.25MPa ($p < 0.05$), but no effect was observed at 0.5MPa ($55\% \pm 14\%$).

To determine if the majority of the DHE staining occurred because of cell death, viability staining was also recorded for each of the stress levels. Results demonstrated that while cell death was increasing, it was not increasing at a rate proportional to the oxidant production (Fig 8).

The percentages of DHE stained cells were seen to increase consistently at each stress level; $3.2\% \pm 3.2\%$ (Control), $12.0\% \pm 9.2\%$ (0.1MPa), $41.1\% \pm 14.4\%$ (0.25MPa), $54.7\% \pm 13.8\%$ (0.5MPa), and $74.9\% \pm 9.2\%$ (1.0MPa).

The percentages of cell death over these same stresses were; $3.9\% \pm 3.2\%$ (Control), $7.4\% \pm 7.2\%$ (0.1MPa), $7.6\% \pm 8.3\%$ (0.25MPa), $12.7\% \pm 8.1\%$ (0.5MPa), and $38.3\% \pm 10.0\%$ (1.0MPa).

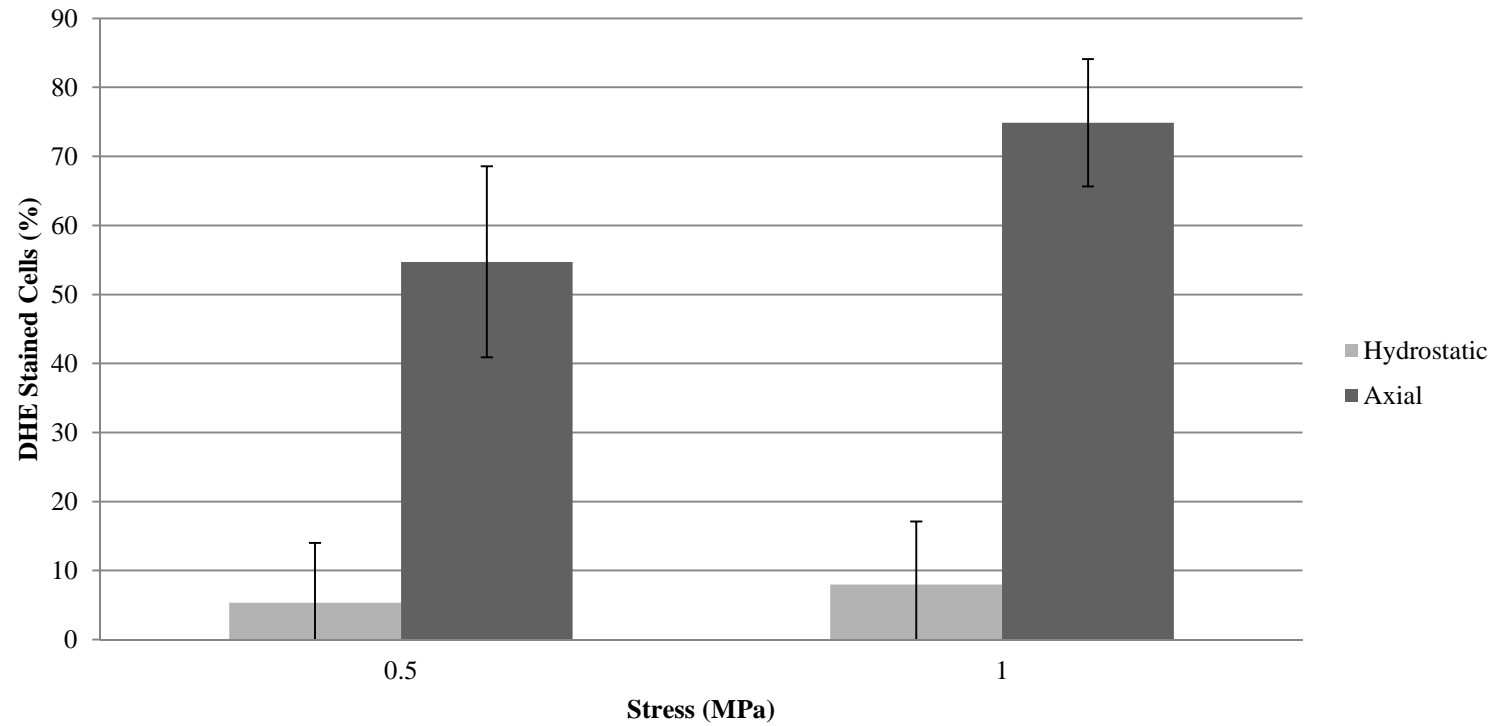


Figure 9. Effects of hydrostatic stress on DHE staining. Hydrostatic stresses (HS) of 0.5 MPa and 1.0 MPa resulted in significantly lower oxidant levels in comparison with 0.5MPa and 1.0MPa of static compressive stress (* $p < 0.05$).

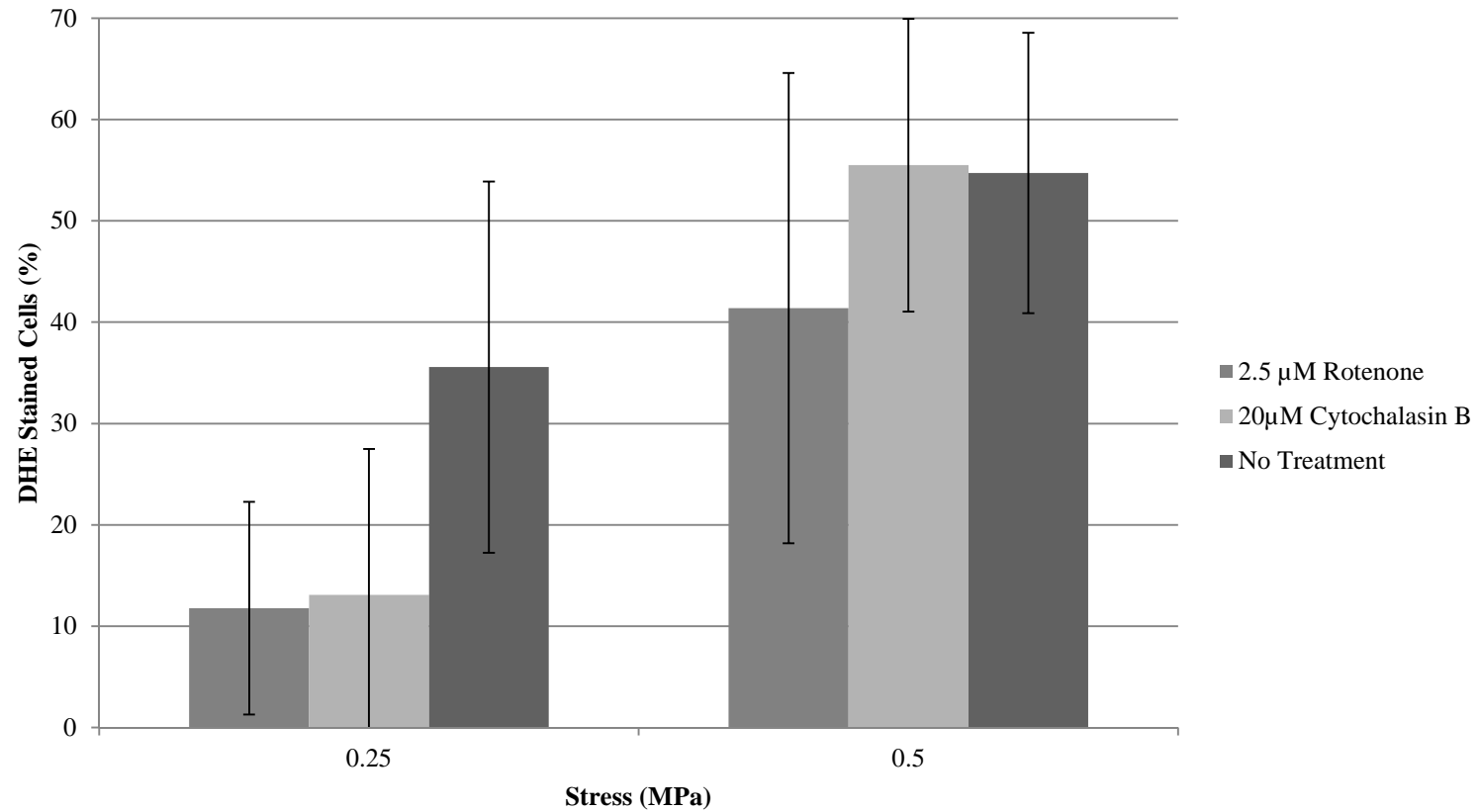


Figure 10. Effects of rotenone and cytochalasin B on stress-induced DHE staining. Inhibition of Mitochondrial electron transport with rotenone decreased oxidant production (% DHE stained cells) after 0.25MPa and 0.5MPa of static compressive stress. Cytoskeletal dissolution with cytochalasin B (Cyto B) significantly decreased DHE at 0.25MPa (* $p < 0.05$) but no reduction was discerned at 0.5MPa.

CHAPTER 5

DISCUSSION

The experimental evidence reported here reveals a strong linear relationship between DHE staining and tissue strain in articular cartilage under static compressive stress at both physiological and super-physiological magnitudes. This response was not observed in cartilage subjected to comparable magnitudes of hydrostatic stress. Together these findings support the hypothesis that physical distortion of chondrocytes, induced by compression, stimulates ROS production.

Rotenone reduced DHE staining under normal compression by 65% at 0.25MPa (Fig 10). This suppressive effect demonstrated that mitochondrial complex 1 (NADH dehydrogenase) was involved in strain-responsive oxidant release. The similar response to cytochalasin B, which reduced DHE staining by 60% at 0.25MPa (Fig 10), indicated that an intact actin cytoskeleton is required for this effect, suggesting a physical link between mitochondria and the cell surface. These results are consistent with published studies showing that filamentous actin transduces tissue-level forces to cell-level strains that are communicated to intracellular organelles and the nucleus [118, 119]. Under normal conditions, mitochondria are firmly attached to filamentous actin [17]. Depolymerizing these actin filaments, using cytochalasin B, detaches mitochondria from the cytoskeleton and results in changes in mitochondrial shape [120].

Due to the nature of the ROS detection technique, these findings do not exclude other sources of cellular ROS. NADPH oxidase and cyclooxygenase are expressed by chondrocytes, and it is possible that these, too, contribute to the ROS detected. Indeed,

production of ROS from alternative sources could explain the observation that rotenone did not reduce DHE staining at strains of greater than 40% (0.5MPa). Alternatively, it is possible that mitochondria were physically damaged by these excessive strains, a process that would lead to increased leakage of oxidants from the electron transport chain.

Further work is needed to better define the response to such super-physiological strains.

The significant stimulatory effects of normal compression on ROS were not observed with hydrostatic compression. This can be explained by the divergent physical effects of the two modes of compression. Articular cartilage is classified as a viscoelastic tissue, which consists of a fluid phase that accounts for 70-80% of its volume [121]. Under normal static compression, outward fluid flow causes solid constituents of the cartilage to consolidate, resulting in tissue strains and chondrocyte distortion. In contrast, cartilage is inherently incompressible under hydrostatic pressure; thus, tissue strains and distortion are theoretically zero.

Physiological strains measured *in vivo* are quite low. For example, 300 seconds after of full body weight static loading, medial and lateral cartilage contact deformation plateau at 12.1% and 14.6%, respectively [122]. In a weight-bearing single leg lunge, deformations in the knee can be seen to reach as high as 30% [123]. These physiological strains are not expected to cause cell death, and this assumption was confirmed by the lack of correlation between cell death and tissue strains <40% in our experiments (0.136; $p=0.361$). However, we did observe that strains > 40% had a positive correlation between ROS release and cell death (0.422; $p=0.0086$). Such extreme physical strains with concomitant chondrocyte attrition are thought to contribute to the development and progression of osteoarthritis [124]. The decreasing mechanical properties shown in

association with osteoarthritis [125] could then be explained in part by a cycle of increasing ROS production and cell death due to increasing strains, though further investigation would be needed to show these changes both *in vivo* and *in vitro*.

ROS participate in a number of broad physiological processes, including responses to pathogens [126] and intracellular signal transduction [127-129]. In chondrocytes, mitochondrial ROS production leads to significant increases in cyclooxygenase activity [130] as well as matrix metalloproteinase 13 (MMP-13), a matrix collagenase [131]. We and others have shown that oxidants play an important role in regulating metabolic activity in cartilage [19, 103]. Previous work showed that 100 μ M tertiary butyl hydroperoxide (tBHP) treatment induced glycolytic activity in cartilage, increasing Hif-1 and GAPDH [106].

There are several limitations to these studies. The first is that only the superficial zone was imaged by confocal microscopy and analyzed. It is therefore not known what the oxidative response of the cells deeper than 200 μ m would be to these conditions. Also the full cartilage tissue strain calculation used for correlating the number of cells stained with DHE does not account for the heterogeneity of strain seen in the tissue. These studies are also a snapshot of the response at one hour after loading. It is unknown what happens to cells after that point. There could be significant cell death from the lower compressive stresses, which is not captured at this time point.

In conclusion, the results of this investigation show that mechanical deformation of cartilage induces mitochondrial strain and ROS release. The strain-dependent release of ROS may be relevant to the observation that physiological mechanical stresses are beneficial to cartilage and increase biosynthetic activity. Since cartilage is an avascular

tissue, with oxygen level estimates ranging from 1% to 6% [99], it depends heavily on glycolysis for ATP production [102]. When cartilage is under anoxic conditions, glycolytic activity declines sharply. This response is termed the *negative Pasteur effect* [102]. Interestingly, the hypoxia-induced inhibition can be reversed by providing exogenous oxidants such as methylene blue [103]. Mitochondrial oxidants also have a key role in maintaining glycolysis in this low oxygen environment. When mitochondrial ROS are blocked in cartilage, ATP levels decline, which can be rescued by addition of external tertiary butyl hydroperoxide [8]. The ROS produced by mitochondria in response to normal mechanical stress might act in a similar manner to support glycolysis, although additional studies of the effects of oxidants and mechanical stresses on ATP production and homeostasis would be needed to test this hypothesis.

REFERENCES

1. Gibson, J.S., et al., *Oxygen and reactive oxygen species in articular cartilage: modulators of ionic homeostasis*. Pflugers Arch, 2008. **455**(4): p. 563-73.
2. Wong, M. and D.R. Carter, *Articular cartilage functional histomorphology and mechanobiology: a research perspective*. Bone, 2003. **33**(1): p. 1-13.
3. Quinn, T.M., et al., *Mechanical compression alters proteoglycan deposition and matrix deformation around individual cells in cartilage explants*. J Cell Sci, 1998. **111** (Pt 5): p. 573-83.
4. Quinn, T.M., V. Morel, and J.J. Meister, *Static compression of articular cartilage can reduce solute diffusivity and partitioning: implications for the chondrocyte biological response*. J Biomech, 2001. **34**(11): p. 1463-9.
5. Stevens, A.L., et al., *Mechanical injury and cytokines cause loss of cartilage integrity and upregulate proteins associated with catabolism, immunity, inflammation, and repair*. Mol Cell Proteomics, 2009. **8**(7): p. 1475-89.
6. Torzilli, P.A., X.H. Deng, and M. Ramcharan, *Effect of compressive strain on cell viability in statically loaded articular cartilage*. Biomech Model Mechanobiol, 2006. **5**(2-3): p. 123-32.
7. Tomiyama, T., et al., *Cyclic compression loaded on cartilage explants enhances the production of reactive oxygen species*. J Rheumatol, 2007. **34**(3): p. 556-62.
8. Martin, J.A., et al., *Mitochondrial electron transport and glycolysis are coupled in articular cartilage*. Osteoarthritis Cartilage, 2012. **20**(4): p. 323-9.
9. Blanco, F.J., I. Rego, and C. Ruiz-Romero, *The role of mitochondria in osteoarthritis*. Nat Rev Rheumatol, 2011. **7**(3): p. 161-9.
10. Zhang, Q., et al., *Circulating mitochondrial DAMPs cause inflammatory responses to injury*. Nature, 2010. **464**(7285): p. 104-7.
11. Coskun, P., et al., *A mitochondrial etiology of Alzheimer and Parkinson disease*. Biochim Biophys Acta, 2011.
12. Gilmer, L.K., et al., *Early mitochondrial dysfunction after cortical contusion injury*. J Neurotrauma, 2009. **26**(8): p. 1271-80.
13. Hartings, J.A., et al., *Spreading depolarizations and late secondary insults after traumatic brain injury*. J Neurotrauma, 2009. **26**(11): p. 1857-66.

14. Sullivan, P.G., M.B. Thompson, and S.W. Scheff, *Cyclosporin A attenuates acute mitochondrial dysfunction following traumatic brain injury*. *Exp Neurol*, 1999. **160**(1): p. 226-34.
15. Chance, B. and G.R. Williams, *Respiratory enzymes in oxidative phosphorylation. I. Kinetics of oxygen utilization*. *J Biol Chem*, 1955. **217**(1): p. 383-93.
16. Goodwin, W., et al., *Rotenone prevents impact-induced chondrocyte death*. *J Orthop Res*, 2010. **28**(8): p. 1057-63.
17. Boldogh, I.R., et al., *A protein complex containing Mdm10p, Mdm12p, and Mmm1p links mitochondrial membranes and DNA to the cytoskeleton-based segregation machinery*. *Mol Biol Cell*, 2003. **14**(11): p. 4618-27.
18. Knight, M.M., et al., *Chondrocyte deformation induces mitochondrial distortion and heterogeneous intracellular strain fields*. *Biomech Model Mechanobiol*, 2006. **5**(2-3): p. 180-91.
19. Sauter, E., et al., *Cytoskeletal dissolution blocks oxidant release and cell death in injured cartilage*. *J Orthop Res*, 2011.
20. Bhosale, A.M. and J.B. Richardson, *Articular cartilage: structure, injuries and review of management*. *Br Med Bull*, 2008. **87**: p. 77-95.
21. Stockwell, R.A., *The cell density of human articular and costal cartilage*. *J Anat*, 1967. **101**(Pt 4): p. 753-63.
22. Becerra, J., et al., *Articular cartilage: structure and regeneration*. *Tissue Eng Part B Rev*, 2010. **16**(6): p. 617-27.
23. Burgeson, R.E., et al., *Human cartilage collagens. Comparison of cartilage collagens with human type V collagen*. *J Biol Chem*, 1982. **257**(13): p. 7852-6.
24. Eyre, D., *Collagen of articular cartilage*. *Arthritis Res*, 2002. **4**(1): p. 30-5.
25. Poole, A.R., et al., *Composition and structure of articular cartilage: a template for tissue repair*. *Clin Orthop Relat Res*, 2001(391 Suppl): p. S26-33.
26. Roughley, P.J., *The structure and function of cartilage proteoglycans*. *Eur Cell Mater*, 2006. **12**: p. 92-101.
27. Morgelin, M., et al., *Cartilage proteoglycans. Assembly with hyaluronate and link protein as studied by electron microscopy*. *Biochem J*, 1988. **253**(1): p. 175-85.

28. Wu, J.P., T.B. Kirk, and M.H. Zheng, *Study of the collagen structure in the superficial zone and physiological state of articular cartilage using a 3D confocal imaging technique*. J Orthop Surg Res, 2008. **3**: p. 29.
29. Weiss, C., L. Rosenberg, and A.J. Helfet, *An ultrastructural study of normal young adult human articular cartilage*. J Bone Joint Surg Am, 1968. **50**(4): p. 663-74.
30. Jeffery, A.K., et al., *Three-dimensional collagen architecture in bovine articular cartilage*. J Bone Joint Surg Br, 1991. **73**(5): p. 795-801.
31. Akizuki, S., et al., *Tensile properties of human knee joint cartilage: I. Influence of ionic conditions, weight bearing, and fibrillation on the tensile modulus*. J Orthop Res, 1986. **4**(4): p. 379-92.
32. Kempson, G.E., et al., *The tensile properties of the cartilage of human femoral condyles related to the content of collagen and glycosaminoglycans*. Biochim Biophys Acta, 1973. **297**(2): p. 456-72.
33. Venn, M.F., *Variation of chemical composition with age in human femoral head cartilage*. Ann Rheum Dis, 1978. **37**(2): p. 168-74.
34. Poole, A.R., et al., *Contents and distributions of the proteoglycans decorin and biglycan in normal and osteoarthritic human articular cartilage*. J Orthop Res, 1996. **14**(5): p. 681-9.
35. Schumacher, B.L., et al., *Immunodetection and partial cDNA sequence of the proteoglycan, superficial zone protein, synthesized by cells lining synovial joints*. J Orthop Res, 1999. **17**(1): p. 110-20.
36. Xia, Y., *Averaged and depth-dependent anisotropy of articular cartilage by microscopic imaging*. Semin Arthritis Rheum, 2008. **37**(5): p. 317-27.
37. Guilak, F., et al., *The pericellular matrix as a transducer of biomechanical and biochemical signals in articular cartilage*. Ann N Y Acad Sci, 2006. **1068**: p. 498-512.
38. Poole, C.A., S. Ayad, and J.R. Schofield, *Chondrons from articular cartilage: I. Immunolocalization of type VI collagen in the pericellular capsule of isolated canine tibial chondrons*. J Cell Sci, 1988. **90** (Pt 4): p. 635-43.
39. Poole, C.A., et al., *Chondrons from articular cartilage (II): Analysis of the glycosaminoglycans in the cellular microenvironment of isolated canine chondrons*. Connect Tissue Res, 1990. **24**(3-4): p. 319-30.

40. Poole, C.A., T.T. Glant, and J.R. Schofield, *Chondrons from articular cartilage. (IV). Immunolocalization of proteoglycan epitopes in isolated canine tibial chondrons*. J Histochem Cytochem, 1991. **39**(9): p. 1175-87.
41. Poole, C.A., et al., *Immunolocalization of type IX collagen in normal and spontaneously osteoarthritic canine tibial cartilage and isolated chondrons*. Osteoarthritis Cartilage, 1997. **5**(3): p. 191-204.
42. Poole, C.A., M.H. Flint, and B.W. Beaumont, *Chondrons in cartilage: ultrastructural analysis of the pericellular microenvironment in adult human articular cartilages*. J Orthop Res, 1987. **5**(4): p. 509-22.
43. Lee, G.M., et al., *Isolated chondrons: a viable alternative for studies of chondrocyte metabolism in vitro*. Osteoarthritis Cartilage, 1997. **5**(4): p. 261-74.
44. Hynes, R.O., *The emergence of integrins: a personal and historical perspective*. Matrix Biol, 2004. **23**(6): p. 333-40.
45. Tamkun, J.W., et al., *Structure of integrin, a glycoprotein involved in the transmembrane linkage between fibronectin and actin*. Cell, 1986. **46**(2): p. 271-82.
46. Takada, Y., X. Ye, and S. Simon, *The integrins*. Genome Biol, 2007. **8**(5): p. 215.
47. Geiger, B., J.P. Spatz, and A.D. Bershadsky, *Environmental sensing through focal adhesions*. Nat Rev Mol Cell Biol, 2009. **10**(1): p. 21-33.
48. van der Kraan, P.M., et al., *Interaction of chondrocytes, extracellular matrix and growth factors: relevance for articular cartilage tissue engineering*. Osteoarthritis Cartilage, 2002. **10**(8): p. 631-7.
49. SALTER, D.M., et al., *INTEGRIN EXPRESSION BY HUMAN ARTICULAR CHONDROCYTES*. Rheumatology, 1992. **31**(4): p. 231-234.
50. Enomoto, M., et al., *Beta 1 integrins mediate chondrocyte interaction with type I collagen, type II collagen, and fibronectin*. Exp Cell Res, 1993. **205**(2): p. 276-85.
51. Durr, J., et al., *Localization of beta 1-integrins in human cartilage and their role in chondrocyte adhesion to collagen and fibronectin*. Exp Cell Res, 1993. **207**(2): p. 235-44.
52. Camper, L., U. Hellman, and E. Lundgren-Akerlund, *Isolation, cloning, and sequence analysis of the integrin subunit alpha10, a beta1-associated collagen binding integrin expressed on chondrocytes*. J Biol Chem, 1998. **273**(32): p. 20383-9.

53. Cao, L., et al., *beta-Integrin-collagen interaction reduces chondrocyte apoptosis*. Matrix Biol, 1999. **18**(4): p. 343-55.
54. Kurtis, M.S., et al., *Integrin-mediated adhesion of human articular chondrocytes to cartilage*. Arthritis Rheum, 2003. **48**(1): p. 110-8.
55. Aguiar, D.J., W. Knudson, and C.B. Knudson, *Internalization of the hyaluronan receptor CD44 by chondrocytes*. Exp Cell Res, 1999. **252**(2): p. 292-302.
56. Reid, D.L., M.B. Aydelotte, and J. Mollenhauer, *Cell attachment, collagen binding, and receptor analysis on bovine articular chondrocytes*. J Orthop Res, 2000. **18**(3): p. 364-73.
57. Fletcher, D.A. and R.D. Mullins, *Cell mechanics and the cytoskeleton*. Nature, 2010. **463**(7280): p. 485-92.
58. Benjamin, M., C.W. Archer, and J.R. Ralphs, *Cytoskeleton of cartilage cells*. Microsc Res Tech, 1994. **28**(5): p. 372-7.
59. Ono, S., *Mechanism of depolymerization and severing of actin filaments and its significance in cytoskeletal dynamics*. Int Rev Cytol, 2007. **258**: p. 1-82.
60. Pollard, T.D. and G.G. Borisy, *Cellular motility driven by assembly and disassembly of actin filaments*. Cell, 2003. **112**(4): p. 453-65.
61. Trickey, W.R., T.P. Vail, and F. Guilak, *The role of the cytoskeleton in the viscoelastic properties of human articular chondrocytes*. J Orthop Res, 2004. **22**(1): p. 131-9.
62. Valiron, O., N. Caudron, and D. Job, *Microtubule dynamics*. Cell Mol Life Sci, 2001. **58**(14): p. 2069-84.
63. Thyberg, J. and S. Moskalewski, *Role of microtubules in the organization of the Golgi complex*. Exp Cell Res, 1999. **246**(2): p. 263-79.
64. Vale, R.D., *Intracellular transport using microtubule-based motors*. Annu Rev Cell Biol, 1987. **3**: p. 347-78.
65. Erdelyi, M., et al., *Requirement for Drosophila cytoplasmic tropomyosin in oskar mRNA localization*. Nature, 1995. **377**(6549): p. 524-7.
66. Langelier, E., et al., *The chondrocyte cytoskeleton in mature articular cartilage: structure and distribution of actin, tubulin, and vimentin filaments*. J Histochem Cytochem, 2000. **48**(10): p. 1307-20.

67. Silberberg, Y.R., et al., *Mitochondrial displacements in response to nanomechanical forces*. J Mol Recognit, 2008. **21**(1): p. 30-6.
68. Grodzinsky, A.J., et al., *Cartilage tissue remodeling in response to mechanical forces*. Annu Rev Biomed Eng, 2000. **2**: p. 691-713.
69. Kuster, M.S., et al., *Joint load considerations in total knee replacement*. J Bone Joint Surg Br, 1997. **79**(1): p. 109-13.
70. Thambyah, A., B.P. Pereira, and U. Wyss, *Estimation of bone-on-bone contact forces in the tibiofemoral joint during walking*. Knee, 2005. **12**(5): p. 383-8.
71. Hodge, W.A., et al., *Contact pressures in the human hip joint measured in vivo*. Proc Natl Acad Sci U S A, 1986. **83**(9): p. 2879-83.
72. Jones, G., K. Bennell, and F.M. Cicuttini, *Effect of physical activity on cartilage development in healthy kids*. Br J Sports Med, 2003. **37**(5): p. 382-3.
73. Manninen, P., et al., *Physical exercise and risk of severe knee osteoarthritis requiring arthroplasty*. Rheumatology (Oxford), 2001. **40**(4): p. 432-7.
74. Palmoski, M., E. Perricone, and K.D. Brandt, *Development and reversal of a proteoglycan aggregation defect in normal canine knee cartilage after immobilization*. Arthritis Rheum, 1979. **22**(5): p. 508-17.
75. Sah, R.L., et al., *Biosynthetic response of cartilage explants to dynamic compression*. J Orthop Res, 1989. **7**(5): p. 619-36.
76. Wang, N., J.P. Butler, and D.E. Ingber, *Mechanotransduction across the cell surface and through the cytoskeleton*. Science, 1993. **260**(5111): p. 1124-7.
77. Loeser, R.F., *Integrin-mediated attachment of articular chondrocytes to extracellular matrix proteins*. Arthritis Rheum, 1993. **36**(8): p. 1103-10.
78. Loeser, R.F., *Modulation of integrin-mediated attachment of chondrocytes to extracellular matrix proteins by cations, retinoic acid, and transforming growth factor beta*. Exp Cell Res, 1994. **211**(1): p. 17-23.
79. Salter, D.M., J.L. Godolphin, and M.S. Gourlay, *Chondrocyte heterogeneity: immunohistologically defined variation of integrin expression at different sites in human fetal knees*. J Histochem Cytochem, 1995. **43**(4): p. 447-57.
80. Knight, M.M., et al., *Mechanical compression and hydrostatic pressure induce reversible changes in actin cytoskeletal organisation in chondrocytes in agarose*. J Biomech, 2006. **39**(8): p. 1547-51.

81. Guilak, F., *Compression-induced changes in the shape and volume of the chondrocyte nucleus*. J Biomech, 1995. **28**(12): p. 1529-41.
82. Meyer, E.G., et al., *Tibiofemoral contact pressures and osteochondral microtrauma during anterior cruciate ligament rupture due to excessive compressive loading and internal torque of the human knee*. Am J Sports Med, 2008. **36**(10): p. 1966-77.
83. Arendt, E. and R. Dick, *Knee injury patterns among men and women in collegiate basketball and soccer. NCAA data and review of literature*. Am J Sports Med, 1995. **23**(6): p. 694-701.
84. Fransen, M., S. McConnell, and M. Bell, *Therapeutic exercise for people with osteoarthritis of the hip or knee. A systematic review*. J Rheumatol, 2002. **29**(8): p. 1737-45.
85. Vasan, N., *Effects of physical stress on the synthesis and degradation of cartilage matrix*. Connect Tissue Res, 1983. **12**(1): p. 49-58.
86. Ng, N.T., K.C. Heesch, and W.J. Brown, *Strategies for Managing Osteoarthritis*. Int J Behav Med, 2011.
87. Haapala, J., et al., *Incomplete restoration of immobilization induced softening of young beagle knee articular cartilage after 50-week remobilization*. Int J Sports Med, 2000. **21**(1): p. 76-81.
88. Hagiwara, Y., et al., *Changes of articular cartilage after immobilization in a rat knee contracture model*. J Orthop Res, 2009. **27**(2): p. 236-42.
89. Haapala, J., et al., *Remobilization does not fully restore immobilization induced articular cartilage atrophy*. Clin Orthop Relat Res, 1999(362): p. 218-29.
90. Hinterwimmer, S., et al., *Cartilage atrophy in the knees of patients after seven weeks of partial load bearing*. Arthritis Rheum, 2004. **50**(8): p. 2516-20.
91. Ikenoue, T., et al., *Mechanoregulation of human articular chondrocyte aggrecan and type II collagen expression by intermittent hydrostatic pressure in vitro*. J Orthop Res, 2003. **21**(1): p. 110-6.
92. Parkkinen, J.J., et al., *Altered Golgi apparatus in hydrostatically loaded articular cartilage chondrocytes*. Ann Rheum Dis, 1993. **52**(3): p. 192-8.
93. Parkkinen, J.J., et al., *Influence of short-term hydrostatic pressure on organization of stress fibers in cultured chondrocytes*. J Orthop Res, 1995. **13**(4): p. 495-502.

94. Falchuk, K.H., E.J. Goetzl, and J.P. Kulka, *Respiratory gases of synovial fluids. An approach to synovial tissue circulatory-metabolic imbalance in rheumatoid arthritis*. Am J Med, 1970. **49**(2): p. 223-31.
95. Ferrell, W.R. and H. Najafipour, *Changes in synovial PO₂ and blood flow in the rabbit knee joint due to stimulation of the posterior articular nerve*. J Physiol, 1992. **449**: p. 607-17.
96. Lund-Olesen, K., *Oxygen tension in synovial fluids*. Arthritis Rheum, 1970. **13**(6): p. 769-76.
97. Najafipour, H. and W.R. Ferrell, *Comparison of synovial PO₂ and sympathetic vasoconstrictor responses in normal and acutely inflamed rabbit knee joints*. Exp Physiol, 1995. **80**(2): p. 209-20.
98. Urban, J.P., *The chondrocyte: a cell under pressure*. Br J Rheumatol, 1994. **33**(10): p. 901-8.
99. Zhou, S., Z. Cui, and J.P. Urban, *Factors influencing the oxygen concentration gradient from the synovial surface of articular cartilage to the cartilage-bone interface: a modeling study*. Arthritis Rheum, 2004. **50**(12): p. 3915-24.
100. Clark, C.C., B.S. Tolin, and C.T. Brighton, *The effect of oxygen tension on proteoglycan synthesis and aggregation in mammalian growth plate chondrocytes*. J Orthop Res, 1991. **9**(4): p. 477-84.
101. Murphy, C.L. and J.M. Polak, *Control of human articular chondrocyte differentiation by reduced oxygen tension*. J Cell Physiol, 2004. **199**(3): p. 451-9.
102. Lee, R.B. and J.P. Urban, *Evidence for a negative Pasteur effect in articular cartilage*. Biochem J, 1997. **321** (Pt 1): p. 95-102.
103. Lee, R.B. and J.P. Urban, *Functional replacement of oxygen by other oxidants in articular cartilage*. Arthritis Rheum, 2002. **46**(12): p. 3190-200.
104. Milner, P.I., R.J. Wilkins, and J.S. Gibson, *The role of mitochondrial reactive oxygen species in pH regulation in articular chondrocytes*. Osteoarthritis Cartilage, 2007. **15**(7): p. 735-42.
105. Fermor, B., et al., *The effects of static and intermittent compression on nitric oxide production in articular cartilage explants*. J Orthop Res, 2001. **19**(4): p. 729-37.
106. Ramakrishnan, P., et al., *Oxidant conditioning protects cartilage from mechanically induced damage*. J Orthop Res, 2010. **28**(7): p. 914-20.

107. Martin, J.A., et al., *N-acetylcysteine inhibits post-impact chondrocyte death in osteochondral explants*. J Bone Joint Surg Am, 2009. **91**(8): p. 1890-7.
108. Buckwalter, J.A. and J.A. Martin, *Osteoarthritis*. Adv Drug Deliv Rev, 2006. **58**(2): p. 150-67.
109. Situnayake, R.D., et al., *Chain breaking antioxidant status in rheumatoid arthritis: clinical and laboratory correlates*. Ann Rheum Dis, 1991. **50**(2): p. 81-6.
110. Grabowski, P.S., et al., *Immunolocalization of inducible nitric oxide synthase in synovium and cartilage in rheumatoid arthritis and osteoarthritis*. Br J Rheumatol, 1997. **36**(6): p. 651-5.
111. Loeser, R.F., et al., *Detection of nitrotyrosine in aging and osteoarthritic cartilage: Correlation of oxidative damage with the presence of interleukin-1beta and with chondrocyte resistance to insulin-like growth factor 1*. Arthritis Rheum, 2002. **46**(9): p. 2349-57.
112. Uesugi, M., K. Yoshida, and H.E. Jasin, *Inflammatory properties of IgG modified by oxygen radicals and peroxynitrite*. J Immunol, 2000. **165**(11): p. 6532-7.
113. Lyyra, T., et al., *In vivo characterization of indentation stiffness of articular cartilage in the normal human knee*. J Biomed Mater Res, 1999. **48**(4): p. 482-7.
114. Franz, T., et al., *In situ compressive stiffness, biochemical composition, and structural integrity of articular cartilage of the human knee joint*. Osteoarthritis Cartilage, 2001. **9**(6): p. 582-92.
115. Bae, W.C., et al., *Indentation testing of human cartilage: sensitivity to articular surface degeneration*. Arthritis Rheum, 2003. **48**(12): p. 3382-94.
116. Ramakrishnan PS, P.D., Stroud NJ, McCabe DJ, Martin JA, *Repeated Measurement of Mechanical Properties in Viable Osteochondral Explants Following a Single Blunt Impact Injury*. Proc Inst Mech Eng(Part H); J Eng Med 2011. **225**(Oct): p. 993-1002.
117. Journot, B.J., Walter, M.W., Martin, J. A., *A Novel System to Automate Image Processing and Analysis for Cell Microscopy*, in *Proceedings of Orthopaedic Research Society 2011*: Long Beach, Ca. p. Poster 1593.
118. Durrant, L.A., et al., *Organisation of the chondrocyte cytoskeleton and its response to changing mechanical conditions in organ culture*. J Anat, 1999. **194** (Pt 3): p. 343-53.

119. Orr, A.W., et al., *Mechanisms of mechanotransduction*. Dev Cell, 2006. **10**(1): p. 11-20.
120. Suelmann, R. and R. Fischer, *Mitochondrial movement and morphology depend on an intact actin cytoskeleton in Aspergillus nidulans*. Cell Motil Cytoskeleton, 2000. **45**(1): p. 42-50.
121. Maroudas, A. and P. Bullough, *Permeability of articular cartilage*. Nature, 1968. **219**(5160): p. 1260-1.
122. Hosseini, A., et al., *In-vivo time-dependent articular cartilage contact behavior of the tibiofemoral joint*. Osteoarthritis Cartilage, 2010. **18**(7): p. 909-16.
123. Bingham, J.T., et al., *In vivo cartilage contact deformation in the healthy human tibiofemoral joint*. Rheumatology (Oxford), 2008. **47**(11): p. 1622-7.
124. Ding, L., et al., *Mechanical impact induces cartilage degradation via mitogen activated protein kinases*. Osteoarthritis Cartilage, 2010. **18**(11): p. 1509-17.
125. Kiviranta, P., et al., *Indentation diagnostics of cartilage degeneration*. Osteoarthritis Cartilage, 2008. **16**(7): p. 796-804.
126. Pillay, J., et al., *Functional heterogeneity and differential priming of circulating neutrophils in human experimental endotoxemia*. Journal of leukocyte biology, 2010. **88**(1): p. 211-20.
127. Benassi, B., et al., *c-Myc phosphorylation is required for cellular response to oxidative stress*. Molecular cell, 2006. **21**(4): p. 509-19.
128. Burgering, B.M. and G.J. Kops, *Cell cycle and death control: long live Forkheads*. Trends in biochemical sciences, 2002. **27**(7): p. 352-60.
129. St-Pierre, J., et al., *Suppression of reactive oxygen species and neurodegeneration by the PGC-1 transcriptional coactivators*. Cell, 2006. **127**(2): p. 397-408.
130. Cillero-Pastor, B., et al., *Mitochondrial dysfunction activates cyclooxygenase 2 expression in cultured normal human chondrocytes*. Arthritis Rheum, 2008. **58**(8): p. 2409-19.
131. Ahmad, R., et al., *Involvement of H-Ras and reactive oxygen species in proinflammatory cytokine-induced matrix metalloproteinase-13 expression in human articular chondrocytes*. Arch Biochem Biophys, 2011. **507**(2): p. 350-5.